Resonant X-Ray Fluorescence Spectroscopy of Correlated Systems: A Probe of Charge-Transfer Excitations

S. M. Butorin,[1,*] D. C. Mancini,[1,†] J.-H. Guo,[1] N. Wassdahl,[1] J. Nordgren,[1] M. Nakazawa,[2] S. Tanaka,[3]
T. Uozumi,[2] A. Kotani,[2] Y. Ma,[4] K. E. Myano,[5] B. A. Karlin,[6] and D. K. Shuh[7]
[1]*Department of Physics, Uppsala University, Box 530, S-751 21 Uppsala, Sweden*
[2]*Institute for Solid State Physics, University of Tokyo, Roppongi, Minato-ku, Tokyo 106, Japan*
[3]*College of Engineering, University of Osaka Prefecture, Gakuen-cho, Sakai 593, Japan*
[4]*Physics Department, University of Washington, Seattle, Washington 98195*
and MSRC, Pacific Northwest Laboratories, Richland, Washington 99352
[5]*Department of Physics, Brooklyn College, Brooklyn, New York 11210*
[6]*National Institute of Standards and Technology, Gaithersburg, Maryland 20899*
[7]*Chemical Sciences Division, Lawrence Berkeley National Laboratory, Berkeley, California 94720*

(Received 1 November 1995)

X-ray fluorescence spectroscopy with monochromatic photon excitation is presented as a tool for studies of charge-transfer excitations in correlated systems, using CeO_2 and UO_3 as examples. Ce $4f \rightarrow 3d$ and U $5f \rightarrow 3d$ x-ray fluorescence, with excitation near the $3d$ thresholds, probes states as eigenvalues for the ground state Hamiltonian from the Anderson impurity model. Sweeping the excitation energy across $3d$ absorption edges enhances contributions of different electronic configurations to fluorescence so that observed resonances indicate the charge-transfer origin of the absorption satellites. [S0031-9007(96)00691-6]

PACS numbers: 78.70.En, 71.27.+a, 71.28.+d, 78.70.Dm

A degree of localization of the f states which can have both bandlike and localized character is a key point in the description of the electronic structure of rare-earth and actinide systems. While delocalized models based on band theory were proposed to explain ground state [1] and spectroscopic [2] properties, various transport and spectroscopic signs of electron correlation effects are observed even in "itinerant" materials and cannot be fully interpreted within one-electron formalism. As an alternative, localized approach the Anderson impurity model (AIM) is often used [3,4] which treats the f states of a rare-earth or actinide atom as a degenerate impurity level hybridized with the valence band, but neglects the interaction between f levels on different atoms. To describe the ground state, a model Hamiltonian is constructed which includes as parameters the energy of a localized state ε_f, delocalized states ε_v, the hybridization strength V, and the on-site f-f Coulomb interaction U_{ff}. The parameters are optimized by fitting both high-energy spectroscopic and low-energy thermodynamic data [3]. However, these parameters may be renormalized in a different way in high- versus low-energy experiments [5,6]. In this case, those experimental techniques become attractive which can be related to both high-energy and low-energy scale techniques such as valence band resonant x-ray fluorescence spectroscopy (RXFS). In the localized, many-body approach, RXFS is expected to probe the states as eigenvalues of the ground state Hamiltonian via creation or annihilation of a core or hole due to site and symmetry selectivity of RXFS. In this Letter, we explore a potential of RXFS in studies of so-called mixed-valency compounds where the anion $2p \rightarrow$ metal f charge-transfer excitations play an important role and the ground state can be described as a strong mixture of several electronic configurations. Using CeO_2 [4,7–11] and UO_3 [12–15] as systems with strong metal f–O $2p$ hybridization we demonstrate that the localized, many-body approach is appropriate for the description of the resonant x-ray fluorescence (RXF) process and that RXF spectra can be interpreted within the framework of the AIM. We show that it is essential to include the RXF data in spectroscopic analysis for these systems in order to derive a unique set of model parameters.

The measurements on CeO_2 were performed at beam line BW3 of HASYLAB, Hamburg, with a modified SX-700 monochromator [16]. X-ray absorption (XA) spectra at the Ce $3d$ edge were obtained by measuring total electron yield. The Ce $4f$-to-$3d$ RXF spectra were recorded using a grazing-incidence grating spectrometer [17]. The emitted radiation was detected in the vertical plane in the direction perpendicular to that of the incident beam. During RXF (XA) measurements, the resolutions of the monochromator and spectrometer were about 1.6 (0.4) and 2.1 eV, respectively. For UO_3, the experiment was carried out at beam line X24A of NSLS, Brookhaven, using a double-crystal monochromator equipped with Si(111) crystals [18]. The U $5f$-to-$3d$ RXF spectra were obtained using a spectrometer based on a bent Si(111) crystal and a position sensitive proportional detector [19]. The spectrometer was placed in the horizontal plane perpendicular to the incident beam. The resolutions of the monochromator and spectrometer were about 0.5 and 1 eV, respectively. For both UO_3 and CeO_2, the incident angle for the incoming beam was ~20° from the sample surface in order to minimize self-absorption effects [20]. The UO_3

sample was a pressed pellet prepared from 99.8% material obtained from Alpha Products. CeO_2 was pelletized using 5 kbar pressure and the pellet was then fired for 24 h in air at 1575 K.

In the one-electron approach, for the excitation tuned to the threshold or above it, the valence band RXF spectra are expected to appear at the same photon energies (except for the elastic peak) and to sample the partial density of states. Some changes in the spectral shape may be observed though if, for example, momentum conservation [21] is fulfilled. For CeO_2 and UO_3, however, the Ce $4f$-to-$3d$ and U $5f$-to-$3d$ spectral variations (Figs. 1 and 2) occur on a larger energy scale than that (2–3 eV) expected based on one-electron calculations for the f density of states [8,12,22]. The energy of the measured RXF spectra follows the varying excitation energy, thus arguing in favor of a localized, many-body description of the RXF process (the emitted photon energy ω must increase with increasing incident photon energy Ω in accordance with the equation $\Omega + E_g = \omega + E_f$, where E_g and E_f are the energies of the ground and final states, respectively).

Ce $4f$-to-$3d$ RXF spectra of CeO_2 recorded at different Ω near the Ce $3d$ threshold are displayed in Fig. 1. For purely tetravalent Ce, one would expect the RXF spectrum to be basically a single, recombination line appearing at ω equal to Ω as a result of the $4f^0 \rightarrow 3d^9 4f^1 \rightarrow 4f^0$ excitation-deexcitation process. However, due to strong Ce $4f$–O $2p$ hybridization in CeO_2, the initial and intermediate states of the RXF process (Fig. 3) can be mainly described as mixtures of $4f^0$ and $4f^1\underline{v}$ configurations and $3d^9 4f^1$ and $3d^9 4f^2 \underline{v}$ configurations ($\underline{v}$ stands for a hole in the valence band), respectively, so that there are radiative transitions back to the ground state and to charge-transfer excited states. This explains the double-line shape of the RXF spectra of CeO_2. One can notice, however, that the energy separation between these two lines as well as their relative intensities strongly depend on Ω. The observed changes can be attributed to variations in the transition rates to different final states of the RXF process which are the bonding (ground state), nonbonding, and antibonding states between $4f^0$ and $4f^1\underline{v}$ configurations. For CeO_2, the RXF process is schematically shown in Fig. 3. When Ω is set to the main Ce $3d_{5/2}$ and $3d_{3/2}$ XA peaks (884.1 and 902.0 eV) the intermediate state which corresponds to the bonding combination between $3d^9 4f^1$ and $3d^9 4f^2 \underline{v}$ configurations decays predominantly to the bonding and nonbonding final states while the transitions to the antibonding final state constitute only ~5% of the total intensity of the inelastic component. The RXF spectrum consists of the intense recombination peak and the line ~4.5 eV lower in energy and broadened due to the finite

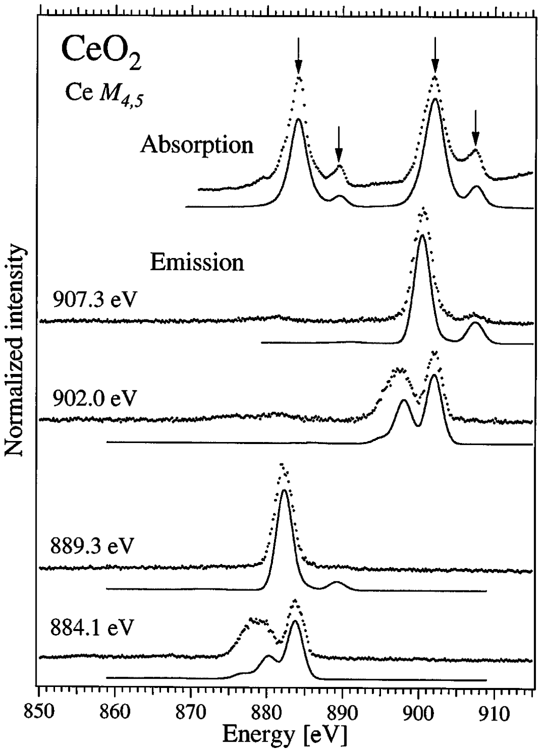

FIG. 1. For CeO_2, the experimental (dots) and calculated (solid lines) Ce $3d$ XA spectrum, and Ce $4f$-to-$3d$ RXF spectra at different excitation energies. RXF data are normalized to the beam monitor reference signal. The arrows on the XA spectrum indicate the excitation energies used for the RXF measurements.

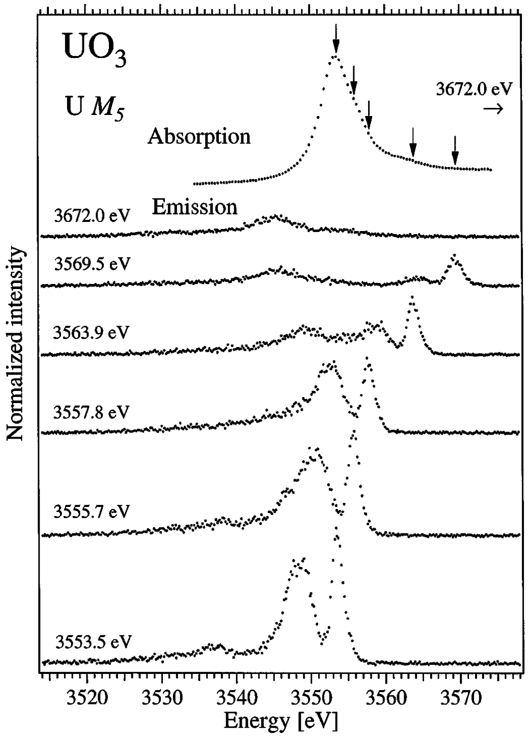

FIG. 2. For UO_3, the U $3d_{5/2}$ XA spectrum, and U $5f$-to-$3d$ RXF spectra recorded at different excitation energies. RXF data are normalized to the beam monitor reference signal. The arrows on the XA spectrum indicate the excitation energies used for the RXF spectra.

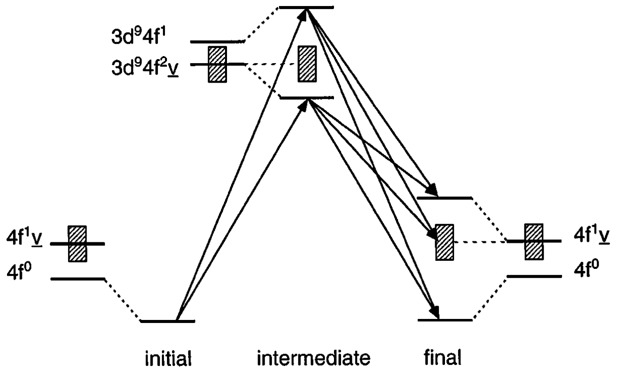

FIG. 3. A schematic representation of the Ce $4f$-to-$3d$ RXF process for CeO_2. Energy levels which are labeled with electronic configurations correspond to the average energies of these configurations in the the limit of $V \to 0$. The shaded rectangles represent the nonbonding states for the $4f^1\underline{v}$ and $3d^94f^2\underline{v}$ configurations.

width of the O $2p$ band. Setting Ω to XA satellites (889.3 and 907.3 eV), which are the antibonding combinations between $3d^94f^1$ and $3d^94f^2\underline{v}$ configurations [4], gives rise to a remarkable enhancement in the relative intensity of the low-energy line which is now ~7 eV below the weak recombination peak. This enhancement can be ascribed to a resonance of antibonding states [23], an indicator of the charge-transfer origin of the XA satellite structures. In this case the transitions to the antibonding final state constitute (80–90)% of the total intensity of the inelastic component. It has been suggested [24] that the XA satellite structures may reflect the extended f states (f continuum). In this case, one would expect a relaxation process leading to the core-hole ionized state and nonresonantlike fluorescence spectra at Ω set to 889.3 and 907.3 eV. Indeed, the low-energy line in the corresponding RXF spectra appears at approximately the same ω as normal fluorescence. However, this low-energy line does exhibit energy dispersion (not shown) with Ω varying through the satellite energy range. The situation is clearer for UO_3 where, for Ω set to a similar charge-transfer satellite (~3563 eV) in the U $3d_{5/2}$ XA spectrum, the resonating low-energy line in the U $5f$-to-$3d$ RXF spectra appears at different ω than that for normal fluorescence. The description of the RXF process in CeO_2, shown in Fig. 3, and corresponding assignments are supported by the results of calculations (Fig. 1) using the AIM.

The RXF spectra were calculated using the expression for the coherent second order optical process given by

$$F(\Omega,\omega)=\sum_f\left|\sum_m \frac{\langle f|T_2|m\rangle\langle m|T_1|g\rangle}{E_g+\Omega-E_m-i\Gamma_m}\right|^2 \times \delta(E_g+\Omega-E_f-\omega)\,, \tag{1}$$

where $|g\rangle$ and $|f\rangle$ are the ground and final states, and $|m\rangle$ is the intermediate state with energy E_m. T_1 and T_2 represent the optical dipole $3d$-to-$4f$ and $4f$-to-$3d$ transitions, respectively. We assumed nonpolarized incident light. The calculations were done including three configurations: $4f^0$, $4f^1\underline{v}$, $4f^2\underline{v}^2$ for $|g\rangle$ and $|f\rangle$, and $3d^94f^1$, $3d^94f^2\underline{v}$, $3d^94f^3\underline{v}^2$ for $|m\rangle$. The effect of multiplet coupling was taken into account in the manner described in Ref. [4]. The values used for the main parameters are as follows: $V = 1.0$, $\varepsilon_f - \varepsilon_v = 2.0$, $U_{ff} = 9.0$, and $U_{fc} = 12.6$ (in units of eV), where ε_v is the center of the valence band assigned a width $W = 2.0$ eV and U_{fc} is the magnitude of the core-hole potential acting on the $4f$ electron. Furthermore, we took into account the configuration-dependent hybridization [25] using two reduction factors $R_c = 0.6$ and $R_v = 0.925$; the hybridization between $3d^94f^1$ and $3d^94f^2\underline{v}$ configurations is taken as R_cV, and that between $4f^1\underline{v}$ and $4f^2\underline{v}^2$ configurations as V/R_v. Since the integrated intensity of the experimental Ce $4f$-to-$3d$ RXF spectra of CeO_2 (Fig. 1) is not proportional to the absorption coefficient at the Ce $3d$ edge due to saturation [26] and self-absorption effects the calculated RXF spectra were simply scaled so as to compare with the experiment.

It is essential to introduce R_c in order to explain the difference in the energy separations between peaks in XA (~5 eV) and 889.3- and 907.3-eV excited RXF (~7 eV) spectra of CeO_2. The actual value of R_c was estimated from a consistent fit of the Ce $3d$ x-ray photoemission, XA, and RXF data of CeO_2 and is found to be in between those for α-Ce and U, respectively, obtained from first principle calculations [25]. The value of $R_v = 0.925$ is not essential for the description of Ce $4f$-to-$3d$ RXF spectra; however, $R_v \sim 0.9$ gives a better fit for the Ce $3d$ x-ray photoemission spectrum. The values of the model parameters used to describe the ground state of CeO_2 are in agreement with those obtained from first principle calculations [8]. The latter calculations reveal strong energy dependence for $|V(\varepsilon)|^2$, being the largest on the top of the O $2p$ valence band. Our V^2 is close to $|V(\varepsilon)|^2$ averaged over ~1.5 eV on the top of the O $2p$ band and the effective width W is almost the same as the energy range which gives a predominant contribution to $|V(\varepsilon)|^2$. Furthermore, using the set of parameters derived in the present analysis the experimental Ce $4d$ XA, valence band photoemission, and bremsstrahlung isochromat spectra of CeO_2 were successfully reproduced [27]. The size of the insulating gap was estimated to be ~4.5 eV, which is in better agreement with experiment than the value of ~2 eV obtained in an earlier analysis [28].

For UO_3, due to the high oxidation state of U (6+), one can expect a significant $5f^2\underline{v}^2$ admixture in the ground state of the system so that this state can be described as a mixture of $5f^0$, $5f^1\underline{v}$, and $5f^2\underline{v}^2$ configurations. In the limit of $V \to 0$, the difference between configuration-averaged energies can be written as $E(5f^1\underline{v}) - E(5f^0) = \Delta$ and $E(5f^2\underline{v}^2) - E(5f^1\underline{v}) = \Delta + U_{ff}$. The specific shape of U $5f$-to-$3d$ RXF spectra for UO_3 (Fig. 2), recorded at Ω set near the U $3d_{5/2}$ threshold, indeed indicates high covalency of chemical bonds in this oxide.

The resonant part of U $5f$-to-$3d$ fluorescence follows Ω due to energy conservation while for Ω set far above the threshold the contribution of nonresonant, normal fluorescence is clearly observed at a constant ω. When Ω is set to satellites in the U $3d_{5/2}$ XA spectrum at about 2–4 and 10 eV above the main XA maximum, one can see some enhancement in the spectral weight of the U $5f$-to-$3d$ fluorescence at about 5, 8.5, and 14.5 eV, respectively, below the recombination line. As in the case of CeO_2, such resonances indicate the charge-transfer origin of satellites (antibonding combinations between $3d^9 5f^1$, $3d^9 5f^2 \underline{v}$, and $3d^9 5f^3 \underline{v}^2$ configurations) in the U $3d_{5/2}$ XA spectrum of UO_3. The most supportive evidence for the idea that the ground state of UO_3 is a mixture of three configurations is the shape of the RXF spectrum recorded at the excitation energy of 3563.9 eV. This spectrum exhibits essentially three lines at about 3563.9, 3558.8, and 3549.4 eV which can be tentatively associated with $5f^0$, $5f^1 \underline{v}$, and $5f^2 \underline{v}^2$ configurations, respectively. The ability to determine from RXF spectra the energies of the states associated with the $5f^2 \underline{v}^2$ configuration puts additional restrictions on the value of U_{ff} for UO_3 because U_{ff} determines the energy of this configuration.

In conclusion, Ce $4f$-to-$3d$ and U $5f$-to-$3d$ RXF spectra of CeO_2 and UO_3 demonstrate that low-energy charge-transfer excitations in correlated systems can be studied by the corresponding core-hole excitation-deexcitation process when there are radiative transitions back to the ground state and low-energy charge-transfer excited states. Because of its site and symmetry selectivity, RXFS allows one to probe Ce $4f$ and U $5f$ states which are basically the eigenvalues of the ground state Hamiltonian in the AIM. The values of model parameters for the ground state of correlated systems can be derived by analyzing the corresponding resonant fluorescence spectra within this model.

We thank Professor L.-G. Johansson for providing the CeO_2 sample and Dr. S. H. Southworth for assistance during measurements on UO_3. This work was supported by the Swedish Natural Science Research Council and Göran Gustavsson Foundation for Research in Natural Science and Medicine. NSLS is operated under contract from DOE.

---

*Present address: MAX-lab, University of Lund, Box 118, S-221 00 Lund, Sweden.

†Present address: Argonne National Laboratory, 9700 South Cass Avenue, APS-XFD/431 Argonne, IL 60439-4812.

[1] For example, B. Johansson and M. S. S. Brooks, in *Handbook on the Physics and Chemistry of Rare-Earths* (North-Holland, Amsterdam, 1993), Vol. 17, p. 149.

[2] For example, M. R. Norman *et al.*, Phys. Rev. Lett. **53**, 1673 (1984); E. Weschke *et al.*, Phys. Rev. Lett. **69**, 1792 (1992).

[3] O. Gunnarsson and K. Schönhammer, Phys. Rev. B **28**, 4315 (1983); O. Gunnarsson *et al.*, J. Appl. Phys. **63**, 3676 (1988).

[4] A. Kotani and H. Ogasawara, J. Electron. Spectrosc. Relat. Phenom. **60**, 257 (1992); Physica (Amsterdam) **186B–188B**, 16 (1993).

[5] O. Gunnarsson and N. E. Christensen, Phys. Rev. B **42**, 2363 (1990).

[6] J. W. Allen and L. Z. Liu, Phys. Rev. B **46**, 5047 (1992).

[7] D. D. Koelling *et al.*, Solid State Commun. **47**, 227 (1983).

[8] A. K. McMahan and R. M. Martin, in *Narrow-Band Phenomena*, edited by J. C. Fuggle, G. A. Sawatzky, and J. W. Allen (Plenum, New York, 1988), p. 133.

[9] A. Fujimori, Phys. Rev. B **28**, 2281 (1983); **28**, 4489 (1983).

[10] E. Wuilloud *et al.*, Phys. Rev. Lett. **53**, 202 (1984).

[11] F. Marabelli and P. Wachter, Phys. Rev. B **36**, 1238 (1987).

[12] M. V. Ryzhkov and V. A. Gubanov, J. Radioanal. Nucl. Chem. **143**, 85 (1990).

[13] B. W. Veal and D. J. Lam, Phys. Lett. **49A**, 466 (1974).

[14] Yu. A. Teterin *et al.*, Phys. Chem. Miner. **7**, 151 (1981).

[15] G. Kalkowski *et al.*, Phys. Rev. B **35**, 2667 (1987).

[16] T. Möller, Synchrotron. Radiat. News **6**, 16 (1993).

[17] J. Nordgren *et al.*, Rev. Sci. Instrum. **60**, 1690 (1989).

[18] P. L. Cowan *et al.*, Nucl. Instrum. Methods Phys. Res., Sect. A **246**, 154 (1986).

[19] S. Brennan *et al.*, Rev. Sci. Instrum. **60**, 2243 (1989).

[20] RXF measurements, performed with two different incident angles (20° and 37°) at some excitation energies, reveal no significant angular dependence for the Ce $4f$-to-$3d$ spectra of CeO_2. This may be connected with the poorly defined surface of the CeO_2 pellet and with specific x-ray detection geometry. In turn, analytical estimates made for the 20° incidence angle indicate that self-absorption leads to the $\sim$25% reduction or to the $\sim$35% enhancement in the integrated-intensity ratio between elastic and inelastic components in the RXF spectra of CeO_2 when the excitation energy is set to the main line or to the satellite, respectively, in the Ce $3d$ XA edges. For UO_3, changes in the shape of RXF spectra caused by self-absorption are found to be less pronounced compared to those for CeO_2 because of the smaller concentration of the f element in UO_3 and larger core-hole lifetime broadening for the U $3d$ edge.

[21] Y. Ma *et al.*, Phys. Rev. Lett. **69**, 2598 (1992).

[22] L. D. Finkelstein *et al.*, Mater. Lett. **14**, 115 (1992).

[23] S. Tanaka *et al.*, J. Phys. Soc. Jpn. **59**, 1488 (1990).

[24] R. C. Karnatak *et al.*, Phys. Rev. B **36**, 1745 (1987).

[25] O. Gunnarsson and O. Jepsen, Phys. Rev. B **38**, 3568 (1988).

[26] For example, S. Eisebitt *et al.*, Phys. Rev. B **47**, 14 103 (1993).

[27] M. Nakazawa, S. Tanaka, T. Uozumi, and A. Kotani (unpublished).

[28] T. Nakano *et al.*, J. Phys. Soc. Jpn. **56**, 2201 (1987).